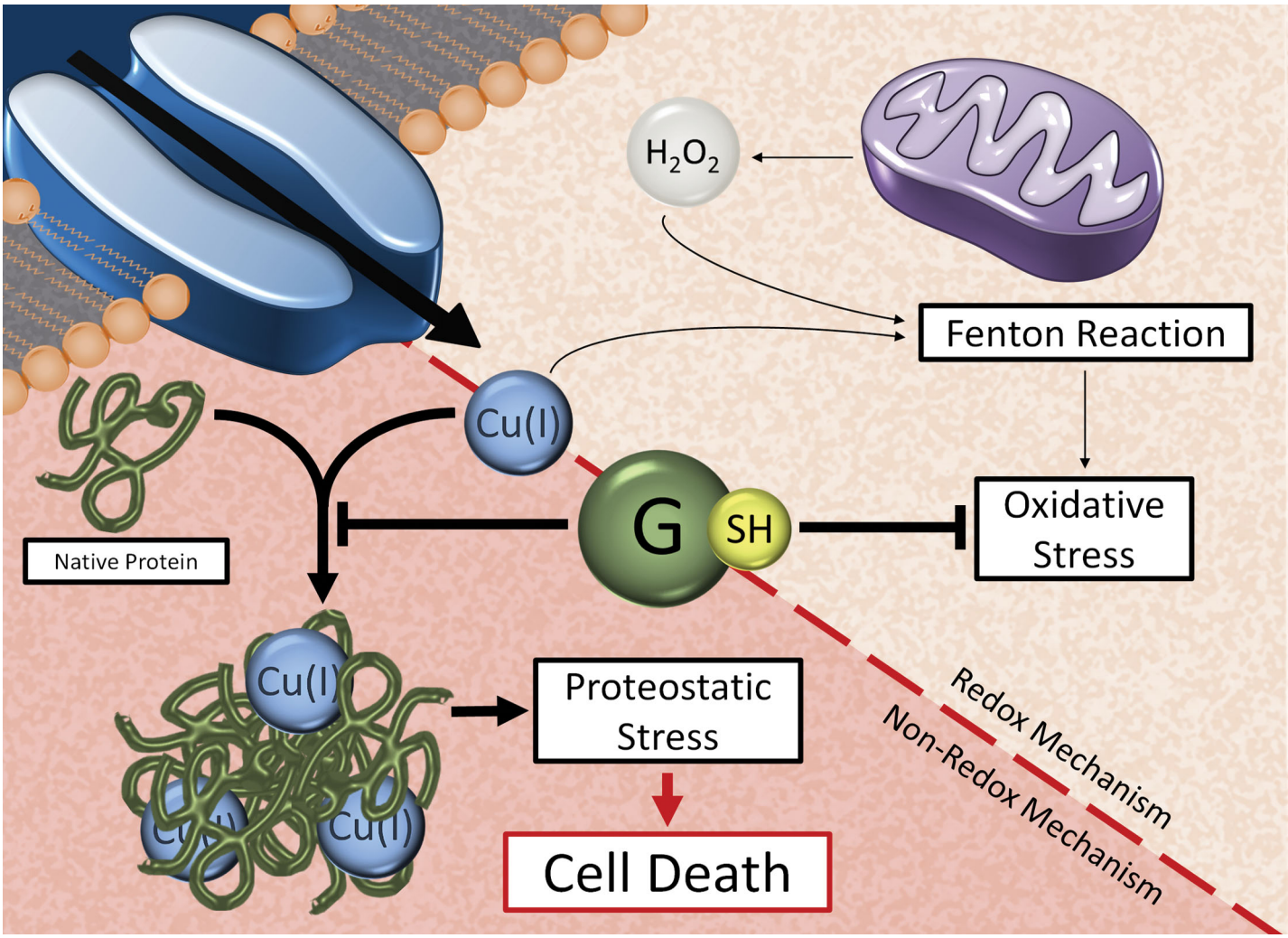

Showcasing research from Professor Dr Marisa Gabriela Repetto laboratory, School of Pharmacy and Biochemistry, University of Buenos Aires, Buenos Aires, Argentina.

Copper-induced cell death and the protective role of glutathione: the implication of impaired protein folding rather than oxidative stress

The cytotoxic mechanism of copper (Cu)-mediated damage that takes place in Wilson disease, in neurologic disorders such as Alzheimer and Parkinson and cancer remains poorly understood. Whereas these pathologies share alterations in cellular redox homeostasis, antioxidant therapies have not provided encouraging results. Here we describe the main mechanism driving cell death due to Cu ions and explain the lack of effectiveness of antioxidant therapies in Cu-related disorders. These insights contribute to better understand the role of Cu in various diseases in order to develop more effective treatment strategies.

As featured in:

See Marisa Gabriela Repetto *et al.*, *Metallomics*, 2018, **10**, 1743.

ROYAL SOCIETY OF CHEMISTRY

rsc.li/metallomics

Registered charity number: 207890

Metallomics

PAPER

Cite this: *Metallomics*, 2018, **10**, 1743

Copper-induced cell death and the protective role of glutathione: the implication of impaired protein folding rather than oxidative stress†

Christian Martín Saporito-Magriñá, [a] Rosario Natalia Musacco-Sebio, [a] Geoffroy Andrieux, [bcd] Lucas Kook, [b] Manuel Tomás Orrego, [e] María Victoria Tuttolomondo, [f] Martín Federico Desimone, [f] Melanie Boerries, [bcdg] Christoph Borner ‡[bh] and Marisa Gabriela Repetto ‡*[ai]

Copper (Cu) is a bioelement essential for a myriad of enzymatic reactions, which when present in high concentration leads to cytotoxicity. Whereas Cu toxicity is usually assumed to originate from the metal's ability to enhance lipid peroxidation, the role of oxidative stress has remained uncertain since no antioxidant therapy has ever been effective. Here we show that Cu overload induces cell death independently of the metal's ability to oxidize the intracellular milieu. In fact, cells neither lose control of their thiol homeostasis until briefly before the onset of cell death, nor trigger a consistent antioxidant response. As expected, glutathione (GSH) protects the cell from Cu-mediated cytotoxicity but, surprisingly, fully independent of its reactive thiol. Moreover, the oxidation state of extracellular Cu is irrelevant as cells accumulate the metal as cuprous ions. We provide evidence that cell death is driven by the interaction of cuprous ions with proteins which impairs protein folding and promotes aggregation. Consequently, cells mostly react to Cu by mounting a heat shock response and trying to restore protein homeostasis. The protective role of GSH is based on the binding of cuprous ions, thus preventing the metal interaction with proteins. Due to the high intracellular content of GSH, it is depleted near the Cu entry site, and hence Cu can interact with proteins and cause aggregation and cytotoxicity immediately below the plasma membrane.

Received 7th July 2018,
Accepted 3rd October 2018

DOI: 10.1039/c8mt00182k

rsc.li/metallomics

Significance to metallomics

Copper (Cu)-mediated damage takes place in Wilson's disease, and has lately drawn attention due to its controversial involvement in neurologic disorders such as Alzheimer's and Parkinson's diseases and cancer. Nonetheless, the cytotoxic mechanism of Cu remains poorly understood. Whereas these pathologies share alterations in cellular redox homeostasis, antioxidant therapies have not provided encouraging results. Here we describe the main mechanism driving cell death due to Cu ions and explain the lack of effectiveness of antioxidant therapies in Cu-related disorders. These insights contribute to better understand the role of Cu in various diseases in order to develop more effective treatment strategies.

[a] *Universidad de Buenos Aires, Facultad de Farmacia y Bioquímica, Departamento de Química Analítica y Fisicoquímica, Cátedra de Química General e Inorgánica, Junin 956, C1113AAD, Buenos Aires, Argentina. E-mail: mrepetto@ffyb.uba.ar*
[b] *Institute of Molecular Medicine and Cell Research, Faculty of Medicine, Albert Ludwigs University of Freiburg, Stefan Meier Strasse 17, D-79104 Freiburg, Germany*
[c] *German Cancer Consortium (DKTK), Partner site Freiburg, Freiburg, Germany*
[d] *German Cancer Research Center (DKFZ), Heidelberg, Germany*
[e] *Universidad de Buenos Aires, Facultad de Farmacia y Bioquímica, Departamento de Fisicomatemática, Cátedra de Física, Junín 956, C1113AAD, Buenos Aires, Argentina*
[f] *Universidad de Buenos Aires, Facultad de Farmacia y Bioquímica, Departamento de Química Analítica y Fisicoquímica, Cátedra de Química Analítica Instrumental, CONICET-UBA, Instituto de Química y Metabolismo del Fármaco (IQUIMEFA), Junín 956, C1113AAD, Buenos Aires, Argentina*
[g] *Comprehensive Cancer Center Freiburg, Faculty of Medicine, Freiburg, Germany*
[h] *Spemann Graduate School of Biology and Medicine, Albert Ludwigs University of Freiburg, Albertstrasse 19a, 79104, Freiburg, Germany*
[i] *Consejo Nacional de Investigaciones Científicas y Técnicas (CONICET), Universidad de Buenos Aires, Facultad de Farmacia y Bioquímica, Buenos Aires, Argentina*

† Electronic supplementary information (ESI) available: This includes Fig. S1 showing microarrays' results in HCT116 cells. See DOI: 10.1039/c8mt00182k

‡ Christoph Borner and Marisa Repetto share senior authorship.

Introduction

Copper (Cu) is an essential trace element in mammalian cells since it is a component of the active site of many enzymes with diverse actions. Under physiological conditions, Cu ions enter cells mainly as Cu(I) by the transmembrane copper transporter 1 (Ctr1)[1] but also as Cu(II) by the divalent metal transporter 1 (DMT1).[2] Once in the cytosol, the chaperone antioxidant protein 1 (Atox1) carries the metal to the pump copper-transporting P-type ATPase (ATP7A/B), where it is incorporated into the *trans*-Golgi network for excretion.[3] Besides Atox1, additional chaperones distribute Cu to the corresponding sites where it is required, ensuring in this manner that free Cu ions are virtually inexistent under physiological conditions.[4]

Wilson's disease (WD) is an inherited disorder characterized by a defective liver Cu-efflux pathway, thus entailing an increased hepatic Cu-content over 20-fold the normal values (50–55 μg g^{-1} organ).[5] Thereby, intracellular Cu accumulation in this pathology triggers cell death.[6] However, the mechanism of cytotoxicity of Cu ions is yet unclear. Furthermore, the underlying cytotoxic mechanisms of several neurodegenerative disorders such as Alzheimer's disease[7–10] or Parkinson's disease[11–13] have been proposed to involve imbalances in Cu homeostasis.

The cytotoxicity of Cu is often attributed to the capacity of Cu(I) to react with hydrogen peroxide (H_2O_2), yielding the highly reactive hydroxyl radical ($HO^{\bullet}$).[14,15] This radical enhances lipid peroxidation and unselectively causes oxidative damage to biomolecules.[16] However, the low selectivity of available methods to measure such short-lived reactive species in biological environments has so far made it difficult to provide experimental evidence for the intracellular formation of this radical.

Different authors have shown a decrease in GSH content upon Cu-overload in cells[17] and in rat liver and brain after acute[18,19] and chronic exposure to the metal.[20–24] However, as the oxidative mechanism of intracellular Cu ions is not fully elucidated, the decreased GSH content could be explained independently of the Cu-oxidizing features, for instance by the presence of dead cells or by a metabolic event preceding cell death. On the other hand, the many reports showing oxidative damage associated with Cu imbalance-related disorders may overshadow the actual role of oxidative stress in the cytotoxic mechanism of Cu ions in metal-overloaded cells. In fact, no antioxidant therapy has ever been able to improve the health condition in these disorders.[25–28] Likely, the redox imbalance induced by Cu overload might have a foremost role in cell signalling, rather than being a driving force of cell death.

The present study was performed to gain a deeper insight into the cytotoxic mechanism of Cu ions and address the relevance of the concomitant oxidative stress. We demonstrate that while Cu overload may enhance intracellular oxidant production, no antioxidant response is observed, and thiol (–SH) homeostasis is not altered in yet living cells. Nonetheless, GSH does protect cells from Cu-induced cytotoxicity, but instead of undergoing oxidation at the –SH group, the peptide binds Cu(I) to prevent the interaction of the metal with protein targets which would otherwise trigger their misfolding and aggregation. Cu-induced cell death is necrotic, although caspases may be activated as a secondary event.

Experimental

Chemicals

Chemicals were purchased from Sigma-Aldrich Chemical Co. (St. Louis, MO). Other reagents were of analytical grade.

Cell culture, copper exposure and preparation of cell extracts

Murine embryonic fibroblasts immortalized with the SV40 T antigen (SV40MEFs), murine hepatoma Hepa1–6 cells, human bronchial epithelial BEAS-2B cells, human colon cancer HCT116 cells, human cervix carcinoma epithelial HeLa cells and murine primary hepatocytes were seeded in 6-well plates as 100 000 cells per well in Dulbecco's Modified Eagle's Medium (DMEM) with 10% fetal calf serum (FCS) and 1% penicillin/streptomycin. Copper exposure was achieved by diluting a $CuSO_4$ stock aqueous solution in the culture medium to obtain the desired final concentration of Cu(II). To prepare cellular extracts, the cells were trypsinized and washed in phosphate buffer solution (PBS). After treatment with lysis buffer (20 mM Tris–HCl, 150 mM NaCl, 5 mM EDTA, 1% Triton X-100, phosphatase inhibitors commercial mix, protease inhibitor cocktail), debris was spin down and the supernatant (cell lysate) was transferred to a new tube.

Cell death analysis

Cells were harvested and washed with PBS followed by incubation with annexin-V-FITC for 15 min. Just before measuring, 7-aminoactinomycin-D (7AAD) was added to the sample. The sample was then measured by flow cytometry (FACS) and four populations could be distinguished: unstained (live cells), 7AAD positive/annexin-V negative (necrotic cells), 7AAD negative/annexin-V positive (apoptotic cells), and 7AAD positive/annexin-V positive (necrotic or late apoptotic cells).[29] Annexin-V-FITC (green) fluorescence was detected by FL-1, and 7AAD fluorescence (red) by FL-3 for 7AAD. Data were acquired with a flow cytometer (FACScalibur, BD Biosciences) and analysed with FlowJo software (Treestar).

Reactive oxygen species (ROS) production

The culture medium was replaced by 10 μM 2′,7′-dichlorofluorescin diacetate (DCFH-DA) (in DMEM). After 45 min incubation (37 °C), the cells were washed in PBS, then trypsinized, and the cell suspension was washed twice at 1200 rpm for 5 min in PBS in FACS tubes. The cells were resuspended in 0.2 mL PBS and analysed by flow cytometry (FACScalibur, BD Biosciences). The fluorescence detected by FL-1 was recorded and data were analysed with FlowJo software (Treestar).[30]

SDS-PAGE and western blot analysis

After resolving the proteins by SDS-PAGE at 200 V for 1 h, they were transferred to a PVDF membrane (400 mA, 60 min) and incubated with antibodies against caspase-3 (1 : 1000) overnight at 4 °C to monitor apoptosis activation. After binding the

secondary antibody (HRP-conjugate 1 : 5000, 1 h at room temperature), the proteins were detected by chemiluminescent autoradiography using a commercial kit, according to the manufacturer's instructions (Amersham, GE Healthcare Sciences). After each antibody-incubation, the PVDF membrane was three times washed for 5 min with PBS 1%, Tween (PBST), and 3% BSA. β-Actin was used as a load control.[31]

Caspase-3 activity

The caspase-3 assay is based in the cleavage of acetyl Asp-Glu-Val-Asp 7-amido-4-methylcoumarin (Ac-DEVD-AMC) by the active enzyme resulting in the release of the fluorescent 7-amino-4-methylcoumarin (AMC).[32] The excitation and emission wavelengths of AMC are 360 nm and 460 nm respectively. A cell lysate was used for the essay and the reaction medium consisted of 20 mM Tris, 150 mM NaCl, 5 mM EDTA, 5 mM sodium pyrophosphate, 1 mM EGTA, 20 mM sodium phosphate monobasic, 3 mM sodium β-glycerophosphate and 10 mM sodium fluoride (pH = 7.4). The protease inhibitor (cocktail, Sigma-Aldrich), MG132 (proteasome inhibitor) and phosphatase inhibitors were added freshly when necessary. 1% dithiotheitrol (DTT) was added to ensure a reduced environment. Fluorescence was recorded for 30 min in a plate reader (Tecan). Results were expressed as relative to the control (%).

Thiol (–SH) group content

The total thiol group content (total –SH) and GSH were determined spectrophotometrically at 412 nm (Tecan) by the formation of the yellow compound 5-thionitrobenzoate (TNB) from 5,5′-dithiobis(2-nitrobenzoic acid) (DTNB).[33] For the determination of total –SH groups, whole cell lysates were employed for the reaction with DTNB. For GSH, the supernatant obtained from a deproteinized (with 0.2 M perchloric acid) cell lysate was neutralized with PBS and then employed for the reaction with DTNB. The determinations were carried out immediately after cell lysis and the samples were kept in ice at all times.

RNA microarrays

BEAS-2B and HCT116 cells were incubated with 800 μM and 1400 μM Cu(II) in the culture medium respectively for different times. At the end of the incubation the cells were harvested for RNA isolation and microarray studies were performed.

To reveal differentially regulated genes in BEAS-2B exposed to Cu overload, we used a linear modelling based approach (limma R/Bioconductor package CITE). Briefly, normalized RNA intensities from duplicated samples at 2, 4, 6, 12 and 18 h following Cu overload were compared to the initial condition at 0 h. We assessed significantly regulated genes using an adjusted *P* value (Benjamini Hochberg) of 0.05. We applied the exact same procedure to get the differentially regulated genes in HCT116 exposed to Cu overload.

The data discussed in this publication have been deposited in NCBI's Gene Expression Omnibus[34] and are accessible through GEO Series accession number GSE109375 (https://www.ncbi.nlm.nih.gov/geo/query/acc.cgi?acc=GSE109375).

Cu content in cells

Cu intake by cells was assessed by atomic absorption[35] in a Buck spectrophotometer; model 210 VGP (BuckScientific, East Norwalk, Connecticut, USA). Cell lysate (0.3 mL) was mineralized in an equal part of 35% hydrogen peroxide and 65% ultrapure nitric acid (HNO_3) (1 : 1) at 60 °C for 90 min. The mixture was then dried at 85 °C overnight. The ashes were dissolved in 0.3 mL 0.1% HNO_3. The atomic absorption of this solution was determined for Cu content in a graphite furnace. The volume of injection was 10 μL. No matrix modifiers were employed. The conditions for Cu determination were: wavelength, 324.7 nm; slit 0.7 nm; current 2 mA, background correction by a deuterium lamp, argon as a protective gas and the peak area as the absorbance measurement. Results were expressed as nmol Cu per mg of protein. Protein content was determined by Bradford's assay.[36]

Cupric ion concentration

The effect of different –SH on the Cu oxidation state was also determined by electron paramagnetic resonance (EPR). The decrease of the signal intensity peaks of Cu(II) in Tris–NaCl buffer (pH 7.4) at 3150.0 G after the addition of different –SH group concentrations was measured as Cu(II) reduction. EPR spectra were recorded at 20 °C using an X-band EPR spectrometer Bruker ECS 106 (Brucker Instruments, Inc., Berlin, Germany). The spectrometer settings were: center field 3200.00 G, sweep width 800.00 G, microwave power 10.0 mW, modulation frequency 50 KHz, modulation amplitude 1.00 G, conversion time 5.15 ms, time constant 5.12 ms, resolution 1024 points.

Cuprous ion concentration

Cu(I) formation from Cu(II) under reducing conditions was assessed by the selective reaction of the former with bicinchoninic acid (Pierce BCA ProteinAssay, Thermo Fisher Scientific). The absorbance at 595 nm was read (Tecan).

Turbidity assay

Tris–HCl 10 mM was used as the reaction medium and stock solutions of 10 mM $CuSO_4{\cdot}5H_2O$, $FeCl_3{\cdot}6H_2O$, $ZnSO_4{\cdot}7H_2O$, $NiSO_4{\cdot}6H_2O$, $MgSO_4{\cdot}7H_2O$, $CoCl_2{\cdot}6H_2O$, $MnSO_4{\cdot}H_2O$, $CaCl_2$ and $CrCl_3{\cdot}6H_2O$ were used so as to attain the desired final concentrations in the wells. 1.5 mg mL^{-1} bovine serum albumin (BSA) was added to the well just before starting the measurement. All the solutions were adjusted to pH 7.4. Samples were incubated and analyzed in a Varioskan Flash 96-well plate reader (Thermo Fisher Scientific) at 37 °C. The absorbance at 405 nm was monitored every 20 s, shaking for 5 s before each measurement during 60 min. No turbidity was detected in the control experiments with buffer only, protein only or metal ions in the absence of protein. Turbidity assays were run at least four times for each condition.[37]

Data analysis

All the results, except for the microarray analyses, are expressed as mean ± standard error of the mean (SEM). Statistical

analyses were carried out with Graphpad InStat following the recommended software settings for the present experiments (Anova with Tukey's post-test). Differences were considered statistically significant at $p < 0.05$. $p < 0.05$, $p < 0.01$ and $p < 0.001$ which were represented as *, ** and ***, respectively, when comparing each condition with the corresponding group.

Results

Cell viability and cell death kinetics after Cu(II) exposure

Several cell lines were studied in order to establish a correlation between the cell sensitivity to Cu overload and oxidative stress-related parameters. Intracellular Cu accumulation may occur due to either decreased efflux of metal ions, *e.g.* in WD, or due to enhanced entrance. The fixed concentration of Cu(II) in the extracellular medium served to set the lag phase before the onset of cell death. As shown in Fig. 1A, when SV40MEF, Hela, BEAS-2B, Hepa1–6 and HCT116 cells were exposed to Cu(II) concentrations (600–2400 μM Cu(II)) for 24 h, they all succumbed to cell death at different metal concentrations. We then chose the Cu(II) concentration which induced 60–80% cell death for each cell line (600 μM for Hela, 600 μM for SV40MEFs, 800 μM for BEAS-2B, 1000 μM for Hepa1–6 and 1400 μM for HCT116) and performed a time kinetic for 0–24 h. As shown in Fig. 1B, the death-kinetics were similar among all cell lines with a lag phase of about 8 h. We therefore used this 8 h lag phase to study the molecular mechanism which might be responsible for the initiation of cell death such as Cu content, the generation of reactive oxygen species, total cellular thiol (–SH) and GSH content and the transcriptional profile of antioxidant enzymes.

Cell death does not correlate with intracellular Cu accumulation and reactive oxygen species production

We measured the intracellular accumulation of Cu by atomic absorption spectrometry. In all cell lines, a similar kinetic of Cu accumulation was observed (Fig. 2A), irrespective of their sensitivity to cell death (compared to Fig. 1A). To measure reactive oxygen species (ROS) production we used dichlorofluorescein (DCFH) as a sensitive but fairly unselective probe for all sorts of oxidant species. Whereas all cells exposed to Cu(II) do show an enhanced DCFH oxidation (Fig. 2B), the rate of DCFH oxidation over a time period of 7 h did not correlate with cell death sensitivity to Cu overload (Fig. 1A). Noticeably, the SV40MEFs showed markedly enhanced ROS production after 3 h of Cu treatment, while in the remaining cells ROS mildly increased after 5–7 h. Therefore, while Cu may enhance oxidant species production, it does not seem to be the main event driving cell death.

Microarray analysis of oxidative stress related genes

We envisaged that if the cellular uptake of Cu triggered ROS production, in particular HO$^{\bullet}$ through the Fenton reaction, the cells would respond to this oxidative stress by transcriptionally upregulating antioxidant enzymes. In order to investigate this, we performed a transcriptome analysis of BEAS-2B cells treated with 800 μM Cu(II) for 2–18 h and assessed the fold change of enzymes involved in the maintenance of redox homeostasis. In detail, this analysis did not reveal any major induction of antioxidant enzymes (Fig. 2C). In fact, the H_2O_2 sink enzymes glutathione peroxidase 8 (GPX8), catalase (CAT) and peroxiredoxin 6 (PRDX6) were even transcriptionally downregulated. Therefore, the reaction between H_2O_2 and Cu(I) is unlikely to drive cell death as cells do not attempt to lower the intracellular concentration of H_2O_2. These results were corroborated in HCT116 cells (see ESI†).

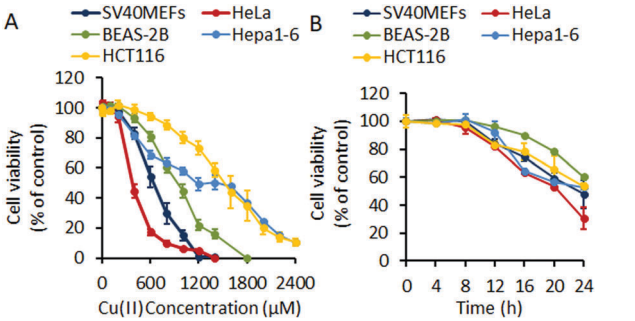

Fig. 1 Cell death induced by Cu overload. (A) Cell viability in different cell lines after 24 h incubation with Cu(II). Error bars represent SEM. $n = 3$. (B) Cell death kinetics in different cell lines incubated with Cu(II). The Cu(II) concentration in the incubation medium for each cell line is as follows: SV40MEFs, 600 μM Cu(II); HeLa, 600 μM Cu(II); BEAS-2B, 800 μM Cu(II); Hepa1–6, 1000 μM Cu(II); HCT116, 1400 μM Cu(II). Error bars represent SEM. $n = 3$.

Total –SH and GSH content does not change in response to Cu treatment

An altered intracellular redox homeostasis involves a change in the ratios of reduced and oxidized –SH groups, especially in GSH/GSSG.[38] Additionally, GSH homeostasis is tightly linked to the metabolic state of the cell, therefore its content should be quantified before the onset of cell death. Indeed, GSH is rapidly depleted in dying cells.[39] Interestingly, our results during the first 7 h of Cu treatment (prior to the onset of cell death) revealed that the cellular content of either total –SH groups (Fig. 2D) or GSH did not significantly change in any of the cell lines tested (Fig. 2E).

We found that Cu(II) could be rapidly reduced to Cu(I) *in vitro* by the –SH groups of *N*-acetylcysteine (NAC), cysteine (Cys) and even GSH (Fig. 2F and G). This result implies that despite the Cu overload, cytosolic Cu is most likely present as Cu(I) because of the high content of reduced GSH in the cells.

GSH but not *N*-acetylcysteine (NAC) is able to protect cells from Cu toxicity

In order to study the role of intracellular –SH groups in the cytotoxicity of Cu ions, the cells were supplemented with NAC. This molecule is employed by cells as a precursor of GSH, enhancing in this manner the intracellular content of this antioxidant.[40] As shown in Fig. 3A, 1–4 mM of NAC was unable to prevent the death of SV40MEFs treated with 600 μM Cu(II) for

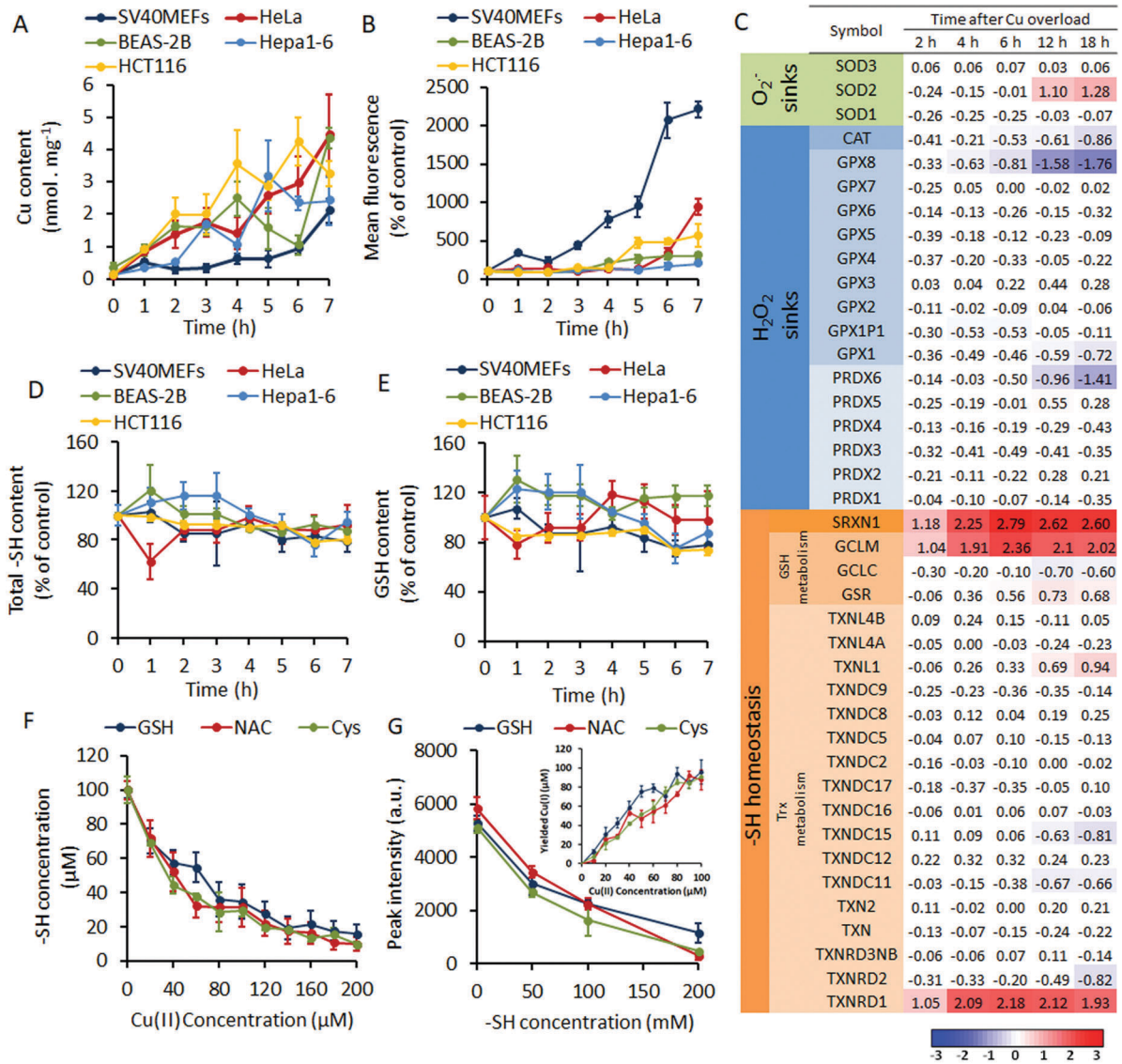

Fig. 2 Redox homeostasis in Cu overloaded cells. In (A–E), cells were exposed to the Cu(II) concentration which killed nearly 50% of the cells at 24 h: SV40MEFs, 600 μM Cu(II); HeLa, 600 μM Cu(II); BEAS-2B, 800 μM Cu(II); Hepa1–6, 1000 μM Cu(II); HCT116, 1400 μM Cu(II). (A) Cu content in different cell lines incubated with Cu(II). Error bars represent SEM. n = 3. (B) DCFH oxidation by different cell lines incubated with Cu(II). Error bars represent SEM. n = 3. (C) Effect of Cu accumulation on the transcriptional profile of antioxidant enzymes in BEAS-2B cells. The concentration of Cu(II) was 800 μM, for the times given. Values correspond to the log 2 fold change. Non-significantly changed values were shown in white. n = 2. (D) Effect of Cu(II) on the total cellular −SH content. Error bars represent SEM. n = 15 for BEAS-2B, n = 9 for HCT 116 and SV40MEFs, n = 6 for HeLa and Hepa1–6. (E) Effect of Cu(II) on the intracellular GSH content. Error bars represent SEM. n = 15 for BEAS-2B, n = 9 for HCT 116 and SV40MEFs, n = 6 for HeLa and Hepa1–6. (F) *In vitro* oxidation of −SH groups on 100 μM GSH, NAC and Cys by Cu(II). Error bars represent SEM. n = 6. (G) *In vitro* reduction of 10 mM Cu(II) by increasing concentrations of GSH, NAC and Cys, assessed by EPR. The intensity on the Y axis corresponds to the characteristic peak observed at ≈3150 G in the Cu(II) spectrum. Error bars represent SEM. n = 3. The embedded graph corresponds to the *in vitro* reduction of Cu(II) by 100 μM GSH, NAC and Cys, assessed by the reaction between Cu(I) and BCA. Error bars represent SEM. n = 3.

24 h, indicating that Cu induced cellular death is not mediated by oxidative stress. Moreover, as the co-treatment with NAC converts Cu(II) into Cu(I) the oxidation state of extracellular Cu seems to be irrelevant for the cytotoxic effect. Therefore, as pointed out above, intracellular Cu(I) most likely kills the cell independent of oxidative stress so that refilling the cytosol with GSH is not important for cell survival. Nonetheless, the addition of either GSH or even GSSG clearly prevented cell death. Noticeably, the addition of GSSG enhanced cell survival roughly twice as efficiently as GSH (Fig. 3A). Due to their peptide nature, GSH and GSSG are unable to passively diffuse through the plasma membrane. Considering that no active uptake of GSH into the cytosol has been reported and the unaltered intracellular GSH content observed here, the similar concentration of exogenous GSH employed to the intracellular concentration of this molecule would hamper the diffusion through facilitated transport. Therefore, their protective effect must be exerted in the extracellular space, most likely by binding Cu

ions and hindering their access to the cytosol. It is worth mentioning that the ratio GSSG/GSH in cytosol[41] is extremely low so despite the fact that the GSSG molecule binds Cu(II), this is not relevant in the intracellular protection against Cu. The formation of Cu-complexes with GSH has been previously reported. However, there is no consensus about which part of the GSH molecule is coordinated to the metal.[42] Given the high intracellular concentration of GSH (1–10 mM), this molecule is expected to perform intracellularly in a very similar manner. In addition, Cu(II) triggered the induction of metallothioneins (Fig. 3B), which are known to actively bind and inactivate metals.[43]

Replenishment of GSH depleted cells with –SH groups does not prevent Cu cytotoxicity

To further study the involvement of GSH and –SH groups in the cytoprotective effect against Cu, we depleted BEAS-2B cells of GSH with buthionine sulfoximine (BSO), which inhibits the enzyme γ-glutamylcysteine synthetase, the rate limiting step in GSH synthesis. Fig. 3C shows that total cellular –SH and GSH diminished after BSO treatment. Concomitantly, the cell viability drastically dropped when the cells were co-treated with BSO and various concentrations of Cu for 24 h (Fig. 3D). Interestingly, replenishment of these cells with –SH groups by the addition of 4 mM NAC did not prevent the increased cytotoxicity of the BSO/Cu co-treatment. While NAC can reduce Cu(II) to Cu(I), it may not bind Cu(I) as strongly as GSH, and thus replenishment of GSH-depleted cells with –SH groups from NAC cannot provide the protection to the same level as GSH. It is worth noticing that the GSH content was nearly ten times greater than the Cu content immediately at the onset of cell death (Fig. 3E) and GSH at mM concentrations buffers free Cu(I) ions to sub-femtomolar concentrations.[44,45]

Microarray analysis reveals that Cu induces genes involved in heat shock (HSR), unfolded protein responses (UPR), ubiquitin/proteasomal degradation and autophagy

We next asked how GSH would protect the cell from Cu cytotoxicity if it were not through its antioxidant function. A closer look at the transcriptome profile in Cu overloaded

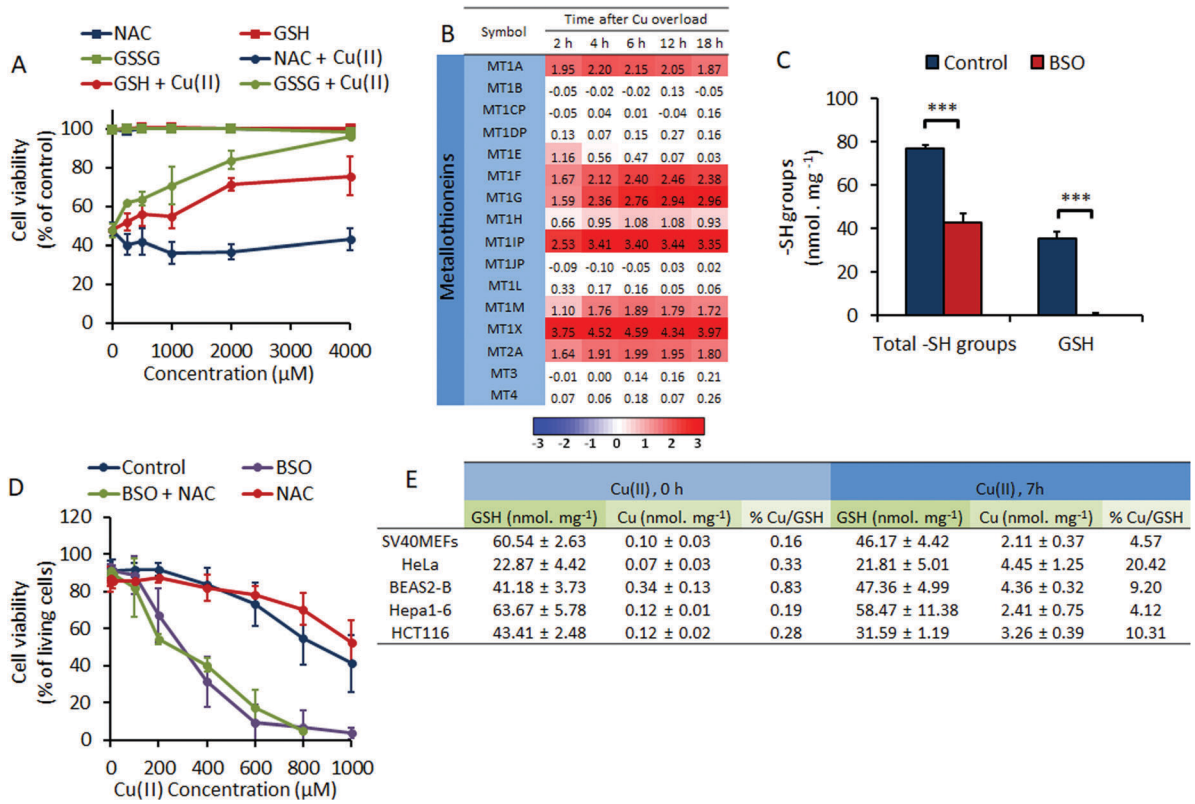

Fig. 3 GSH protection in Cu-overloaded cells. (A) Effect of the exogenous addition of GSH, GSSG or NAC on the cell viability of SV40MEF cells exposed to 600 μM Cu(II) for 24 h. Different concentrations of GSH, GSSG or NAC were added simultaneously with Cu(II). Error bars represent SEM. n = 9. (B) Metallothionein induction in BEAS-2B cells after exposure to 800 μM Cu(II). Values correspond to the log 2 fold change. Non-significantly changed values were shown in white. n = 2. (C) Total –SH groups and GSH content in BEAS-2B cells incubated with 1 mM BSO for 24 h. Error bars represent SEM. n = 3. ***, $p < 0.001$. (D) Effect of GSH depletion by BSO and subsequent replenishment of –SH groups by addition of 4 mM NAC on cell viability in BEAS-2B cells incubated with Cu(II) for 24 h. Cells were depleted from GSH by incubation with 1 mM BSO for 24 h previous to the addition of Cu(II). BSO 1 mM was kept at all times during the incubation with Cu(II). Error bars represent SEM. n = 9 for the control, BSO and BSO + NAC and n = 6 for NAC. (E) Relative Cu to GSH content at the beginning of the incubation and immediately before the onset of cell death. The Cu(II) concentration for each cell line in (E) is as follows: SV40MEFs, 600 μM Cu(II); HeLa, 600 μM Cu(II); BEAS-2B, 800 μM Cu(II); Hepa1–6, 1000 μM Cu(II); HCT116, 1400 μM Cu(II). Values after ± represent SEM. n = 3 for Cu content values; for GSH content, n = 15 for BEAS-2B, n = 9 for HCT 116 and SV40MEFs, n = 6 for HeLa and Hepa1–6.

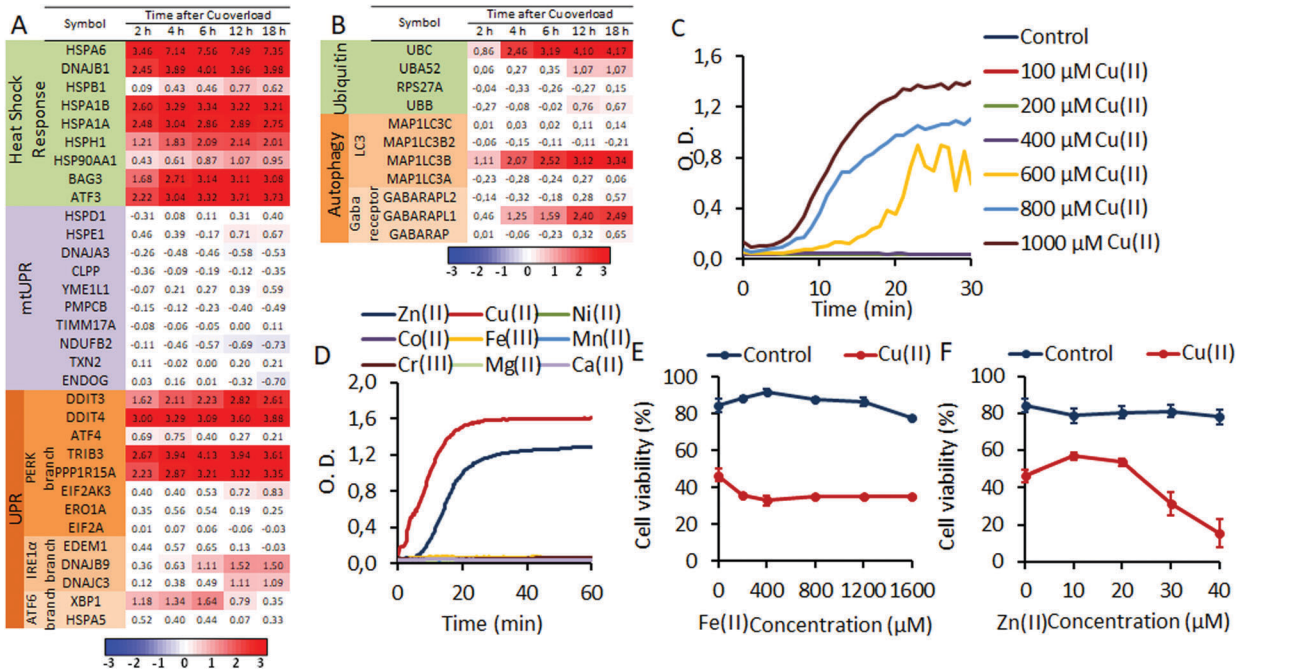

Fig. 4 Effect of Cu overload on cellular proteostasis. (A) Effect of Cu accumulation on the transcriptional profile of HSR, mtUPR and UPR related genes in BEAS-2B cells. (B) Effect of Cu accumulation on the transcriptional profile of autophagy and proteasomal degradation related genes in BEAS-2B cells. The concentration of Cu(II) in (A) and (B) was 800 μM, for the times given. Values in tables correspond to the log 2 fold change. Non-significantly changed values were shown in white. n = 2. (C) Optical density (O.D.) measured at 405 nm of BSA aggregates induced by different concentrations of Cu(II). n = 5. (D) O.D. measured at 405 nm of BSA aggregates induced by different metals. The concentration was 800 μM for each metal. n = 5. (E) Cell viability of SV40MEFs incubated with 800 μM Cu(II) and Fe^{2+} for 24 h. Cu(II) and Fe(II) were added simultaneously at the beginning of the experiment. Error bars represent SEM. n = 3. (F) Cell viability of SV40MEFs incubated with 800 μM Cu(II) and Zn^{2+} for 24 h. Cu(II) and Zn(II) were added simultaneously at the beginning of the experiment. Error bars represent SEM. n = 12.

BEAS-2B cells revealed a consistent and strong activation of the heat shock response (HSR) (Fig. 4A). This response arises from increased levels of improperly folded proteins in the cytosol. An enhanced unfolded protein response (UPR), although milder than the HSR, which originates due to an increased protein load in the endoplasmic reticulum (ER),[46] was also observed (Fig. 4A). However, there was a remarkable lack of mitochondrial UPR (mtUPR) (Fig. 4A), which is induced by increased loads of mitochondrial unfolded proteins.[47] Our findings indicate that Cu overload affects proteostasis especially in cellular compartments which seem to be involved in the efflux pathway of Cu ions such as the cytosol and the ER. In agreement with impaired proteostasis we observed the induction of ubiquitin in our microarray analysis after Cu treatment, pointing towards increased proteasomal degradation of improperly folded proteins (Fig. 4B). Additionally, the autophagic regulators LC3 and GABARAPL1[48] were induced, suggesting that increased autophagy may be used to remove and further degrade misfolded and aggregated protein complexes from the cytosol. These results were corroborated in HCT116 cells (see ESI†).

Cu induces protein aggregation in a time and concentration dependent manner

In agreement with our findings so far, Cu(II) was able to directly induce the aggregation of bovine serum albumin (BSA) *in vitro* in a time and concentration dependent manner (Fig. 4C). This aggregation may be due to covalently cross-linked multimers because of the ability of Cu(II) to oxidize –SH groups on different molecules.[37] However, such a reaction is not critical for Cu cytotoxicity as previously shown (Fig. 3A). Protein oxidation by Cu(II) would mask the aggregation due to direct protein–metal interactions. Nonetheless, BSA possesses only one available reduced –SH group, ruling out the possibility for covalently linked multimer formation. Additionally, it must be mentioned that BSA is a stable protein which does not easily aggregate in contrast to highly disordered intracellular proteins such as α-synuclein. In comparison to other metals, Cu(II) was the most efficient in promoting protein aggregation followed by zinc(II) (Zn(II)) (Fig. 4D). Interestingly, iron(III) (Fe)(III) did not induce protein aggregation. A similar behaviour of metals has been previously reported with γ-D-crystallin.[37]

Zn, but not Fe, potentiates Cu-induced cytotoxicity

Zn and Fe possess different mechanisms of toxicity. Fe participates in the Fenton reaction yielding highly reactive hydroxyl radicals while Zn is unable to do so. We therefore tested if Fe(II) or Zn(II) could potentiate Cu(II)-induced cell death of SV40MEF cells due to the depletion of common metabolic systems. As shown in Fig. 4E and F, while Fe(II) had no effect on Cu(II) toxicity, Zn(II) dramatically potentiated cell death. Although Zn is redox inactive, it shares the folding impairing feature of Cu.[49] This strongly suggests that Cu ions have a direct impact on protein homeostasis which is

tightly linked to the survival of the cell. It will be critical to identify which proteins are being mainly affected by the Cu(I) overload in order to characterize their binding equilibria with the metal.

Both GSH and GSSG prevent Cu-induced protein aggregation

As shown in Fig. 4C, the incubation of BSA with Cu(II) quickly led to the formation of protein aggregates. However, as shown above, Cu is mainly present as Cu(I) after it is taken up by cells. In the presence of NAC, which reduced Cu(II) to Cu(I), protein aggregation still took place but at a slower rate (Fig. 5B). Probably, Cu(II) induced protein aggregation more rapidly than Cu(I) due to the more polarizing feature of the higher oxidation state of the metal but NAC might also weakly bind Cu(I), hindering its interaction with the protein. We then tested if GSH could effectively prevent Cu(II)/Cu(I)-induced protein aggregation (Fig. 5A). As Cu(II) and GSH cannot coexist, the spontaneous reduction of Cu(II) by GSH to Cu(I) will take place. Remarkably, both GSH (Fig. 5A) and GSSG (Fig. 5B) were able to fully prevent Cu(II)/Cu(I)-induced aggregation of BSA *in vitro*. The mechanisms though seem different because GSH will first reduce Cu(II) to Cu(I) and then bind the reduced form of the metal, while GSSG is able to directly bind Cu ions. This indicates that in addition to its known role as an antioxidant, GSH is also able to prevent Cu-induced protein aggregation.

Caspase activation and PARP cleavage

Sustained protein misfolding and aggregation has been shown to trigger cell death by apoptosis or necrosis. Apoptosis is characterized by the activation of caspases, in particular effector caspase-3. The treatment of SV40MEF cells with 600 μM Cu led to a time-dependent increase in caspase-3 activity (Fig. 6A) and procaspase-3 processing into its active p17 form (cleaved caspase-3) (Fig. 6B). Concomitantly, PARP, one of the major caspase-3 substrates, was effectively cleaved (Fig. 6B). As a consequence, a high percentage of Cu-treated cells displayed annexin-V-FITC staining without plasma membrane permeabilization (7AAD co-staining) (Fig. 6D). Some cells however stained positive for both markers (annexin-V and 7AAD) indicating that they underwent necrosis or secondary necrosis after apoptosis. Moreover, although a cellular treatment with the pan-caspase inhibitor zVAD.fmk abrogated Cu-induced caspase-3 activation (Fig. 6C) it did not protect the cells from dying (Fig. 6D). Therefore, the activation of caspases was most likely a secondary event to cell death. Indeed, the morphology of the dead cells was more necrotic rather than apoptotic (Fig. 6E). Moreover, among the cells studied, caspase activation occurred solely in SV40MEFs. This is likely related to the cell transformation of these cells by the SV40 TAg, which may itself influence the kind of cell death signalling seen in these cells.

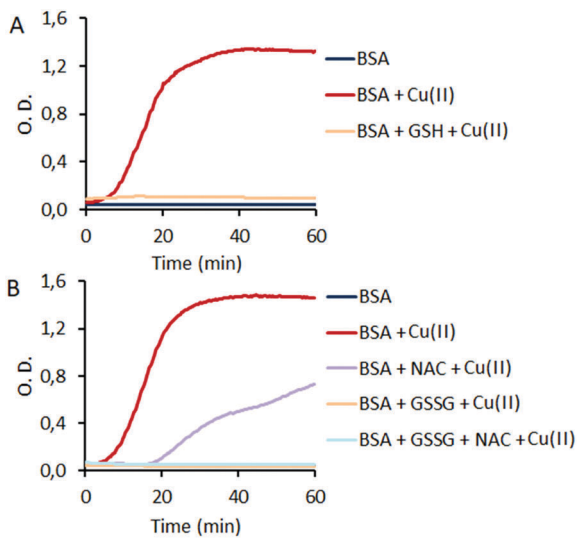

Fig. 5 Protective role of GSH against Cu induced protein aggregation. (A) Inhibition of Cu(II)-induced aggregation of BSA by addition of GSH. The concentrations of the reagents were 800 μM for Cu(II) and 2 mM for GSH. (B) Inhibition of Cu(II) induced aggregation of BSA by addition of GSSG and NAC. The concentrations of the reagents were 800 μM for Cu(II), 2 mM for GSH and 2 mM for NAC. In the group BSA + GSSG + NAC + Cu(II), the reagent NAC was mixed with Cu(II) and then with GSSG to ensure the reduction of the metal.

Discussion

Cu uptake is necessary for cell survival, as these ions are involved in numerous important biological reactions. However, due to its chemical properties, involving both pro-oxidant and pro-aggregating reactions, the accumulation of Cu ions may become highly cytotoxic. Unravelling the events mediating Cu-induced cytotoxicity is critical to understand the cell death mechanism in WD and also to determine the participation of this metal in less understood scenarios such as Alzheimer's disease and Parkinson's disease (Fig. 7).

The accumulation of Cu ions may take place when the efflux of the metal from the cell is impaired, as observed in WD. In this manner, Cu sinks would gradually saturate, culminating in an increase of free Cu ions. In this work, we employed high extracellular concentrations of Cu(II) in order to attain an increased intracellular steady-state of Cu ions. It is worth mentioning that the nearly 20-fold increase of the intracellular Cu content observed here (Fig. 2A) is similar to that in WD model cells with defective Cu extrusion pathways exposed to low concentrations of Cu ions.[50]

The intracellular accumulation of Cu ions enhances the production of oxidant species. However, the lack of a transcriptionally mediated antioxidant response against the built up Cu (Fig. 2C) along with the high content of intracellular GSH (Fig. 2E) suggests that oxidative stress is not the critical event leading to cell death. These parameters were determined prior to the onset of cell death as they are tightly linked to cell metabolism, thus the presence of dead cells might influence the result. The enhanced production of oxidant species induced by Cu-overload is probably involved in intracellular signaling[51] rather than being a driving force of cell death. In contrast, the transcriptional response in Cu-overloaded cells is mainly directed to restore protein homeostasis (Fig. 4A). In line with this observation, Cu(II) and Cu(I) were both able to promote protein

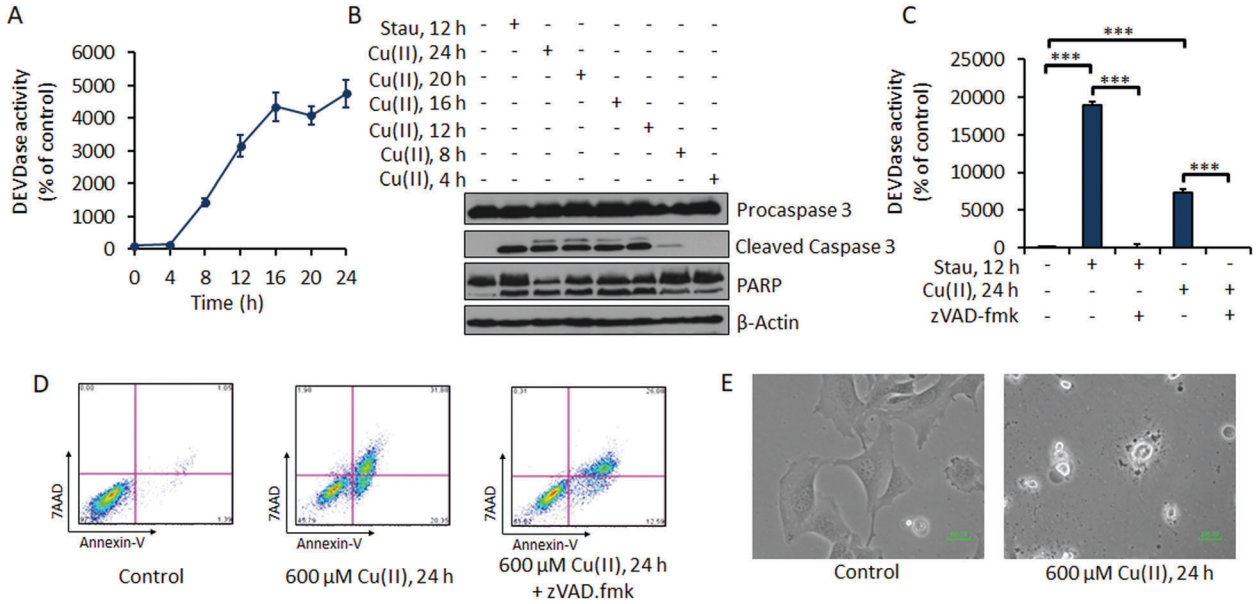

Fig. 6 Role of apoptosis in the cytotoxicity of Cu. (A) Caspase 3/7 activity assessed as DEVDase activity in SV40MEF cells incubated with 600 μM Cu(II). Error bars represent SEM. $n = 2$. (B) Caspase 3 and PARP cleavage in SV40MEF cells incubated with 600 μM Cu(II). $n = 3$. (C) Caspase activity inhibition by 1 μg mL^{-1} zVAD.fmk in SV40MEF cells incubated with 600 μM Cu(II) for 24 h. Error bars represent SEM. $n = 3$. ***, $p < 0.001$. (D) Annexin-V/7AAD staining assessed by flow cytometry in SV40MEF cells incubated with 600 μM Cu(II) for 24 h in the presence and absence of 1 μg mL^{-1} zVAD.fmk. $n = 3$. (E) Cell morphology assessed by light microscopy in SV40MEF cells incubated with 600 μM Cu(II) for 24 h. 1 μg mL^{-1} Stau (Staurosporine) was used as a positive control for apoptosis.

aggregation *in vitro* (Fig. 4C) and the co-incubation of Cu(II) with the pro-aggregating metal Zn(II) (Fig. 4F) potentiated cell death induced by Cu ions whereas the pro-oxidizing metal Fe(II) did not. Regarding the pro-aggregating features of Cu(II), it must be mentioned that the content of intracellular reduced –SH groups is well above that of Cu ions (Fig. 3E), thus maintaining the metal as Cu(I). Nonetheless, Cu(I) also induced protein aggregation. Therefore, the influx of Cu(I)/Cu(II) allows the undesirable metal contact with proteins which impairs protein folding resulting in cytotoxicity, since Cu(I) in cells is mostly in contact with the desirable metal sites in proteins for its function.

Most interestingly, GSH, which is a critical molecule in the control of oxidant stimuli, does protect the cells from Cu ions, but independently of the antioxidant properties of the –SH group of the tripeptide. Rather than as an antioxidant, the –SH group in GSH may act as a key Cu(I) binding ligand that prevents Cu(I) access to the undesirable metal sites in proteins which induces protein aggregation. Interestingly, both GSH and GSSG may bind Cu ions but with different mechanisms because GSH reduces Cu(II) and then may bind yielded Cu(I) while GSSG is able to directly bind Cu ions. In the case of NAC, as it does not strongly bind Cu(I), it is unable to protect the cell from the metal overload (Fig. 3A). It is worth mentioning that the replenishment of –SH groups by addition of NAC after BSO treatment would still hinder the activity of GSH dependent enzymes. Nonetheless, the lack of transcriptionally activated enzymes involved in GSH usage indicates that such reactions are not critical for cell survival. Altogether, our findings suggest two mechanisms by which GSH protects cells from Cu cytotoxicity. GSH prevents protein misfolding caused by the direct interaction with Cu ions while it also may participate in antioxidant pathways. The relevance of each mechanism in Cu cytotoxicity depends on additional stimuli which boost either pro-aggregating or pro-oxidizing reactions.

The molecular events leading to Cu cytoxicity are not homogeneously spread throughout the cell. In fact, they are concentrated in the cytosol and, to a lesser extent, in the endoplasmic reticulum, whereas mitochondria are largely unaffected (Fig. 4A). Considering GSH content is at least ten fold (Fig. 3E) greater than that of intracellular Cu(I) before the onset of cell death, the increment in free Cu(I) available to react with intracellular targets cannot be achieved upon complete titration of intracellular GSH. Indeed, the HSR and UPR start before the first two hours of Cu(II) exposure when the Cu content has barely increased (Fig. 4A). Therefore, we speculate that such reactions are also not homogeneously distributed in the cytosol since GSH would inactivate Cu(I). We rather think that these reactions take place immediately below the membrane site of entrance of the metal ions, where the competition between entering free Cu(I) with either GSH/Atox1, and the incorporation in the trafficking pathways, or with proteins impairing protein folding, or with H_2O_2, leading to oxidative stress, occurs. Thus, the relative concentration of such agents near the influx site will determine the nature of cell death due to Cu ions and the relevance of the therapies applied. In unstressed cells, the role of oxidative stress induced by Cu overload, while present, seems minor. Nonetheless, in specific cells with higher intracellular H_2O_2 steady-state concentrations, the cytotoxicity of Cu ions may shift from impaired proteostasis to oxidative modifications and ensuing cell death. Altogether, these results explain why antioxidant therapies are largely ineffective in Cu imbalance related disorders such as WD, whereas chelating agents remain the first line therapy.

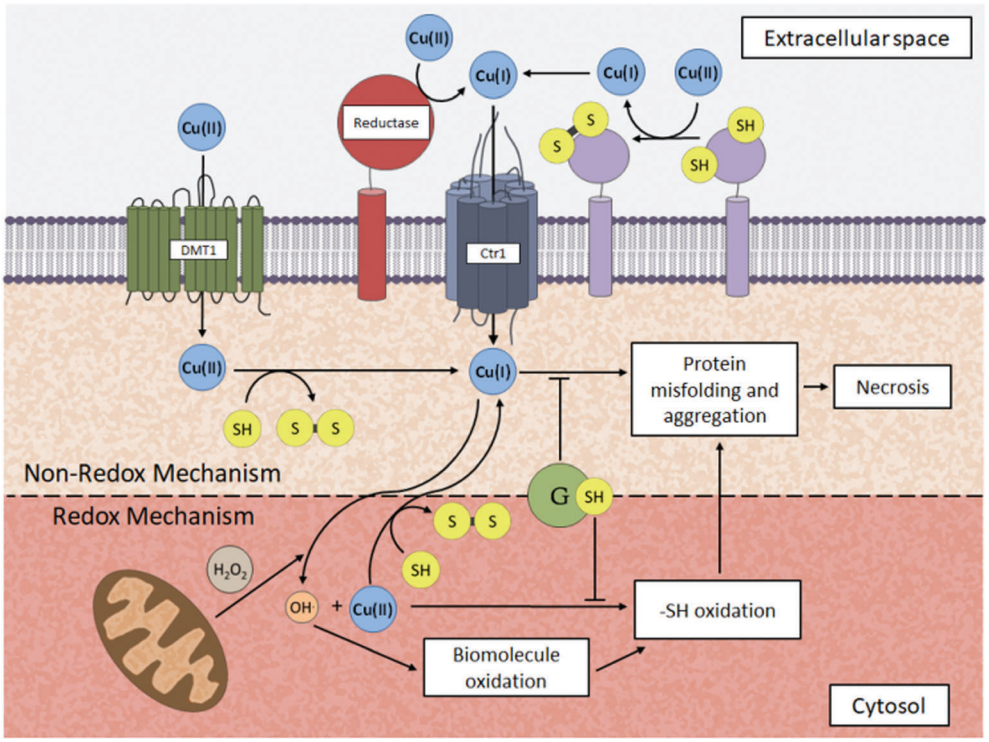

Fig. 7 Cytotoxic mechanism of Cu ions. Cu may be acquired either as Cu(I) by Ctr1 or as Cu(II) by DMT1. In any case, Cu(II) is reduced upon entrance by cytosolic –SH groups. When the rate of Cu(I) uptake is high, the neighbouring GSH at the influx site is titrated by the entering metal, thus allowing Cu(I) to interact with toxic targets. Cu(I) reaction with H_2O_2, while possible, is not relevant since due to the low H_2O_2 concentration, metal ions are more likely to interact directly with proteins. In consequence, Cu(I) induced cell death is driven by the impaired protein folding and likely aggregated proteins. Cell death induced by Cu overload is fully necrotic. In specific conditions, where H_2O_2 is present at a higher steady-state concentration, the nature of cell death may shift from impaired proteostasis to oxidatively modified molecules. Noticeably, GSH actively protects the cell against Cu ions in both the redox-independent mechanism, by means of the coordinating and inactivating feature of the molecule, and in the redox-dependent cell death mechanism, through the reactive –SH group and the GSH dependent enzymes which control redox homeostasis.

Noticeably, increased Cu content has been reported in tumors[52] and this may affect protein homeostasis. In fact, cancer cells are especially sensitive to proteasome inhibitors.[53] While this study highlights the lack of correlation between the sensitivity to Cu ions and oxidative stress in a set of cell lines, the mechanism proposed could be in principle extrapolated to other cell types undergoing Cu overload. Likely, future studies may unravel differences in the cytotoxic mechanism of Cu downstream of the main event driving cell death presented here, due to the spectrum of proteins expressed in each cell and the corresponding chemistry of their direct interaction with Cu ions.

Finally, future implications must be considered since, aside from a mild Cu overload, a second hit impacting on the overall GSH content such as malnutrition,[54] specific stages of development,[55] cell differentiation[56] or even aging cells[57] would entail an additional load for the protein folding machinery due to the direct interaction of Cu(I) with proteins, thus triggering or worsening on-going aggregopathies.

Conclusions

Cu overload in cells leads to cell death, independently of the ability of Cu ions to enhance oxidant production. In fact, Cu accumulation does not alter –SH group homeostasis of yet living cells. Moreover, the metal directly interacts with proteins and elicits cellular responses to restore protein homeostasis. While the antioxidant GSH is a major protective molecule against the toxicity of these ions, the nature of this function is not only based on its redox chemistry but rather on its ability to form an inactive complex with Cu(I), thus preventing the interaction of the metal ions with proteins and the ensuing misfolding or aggregation.

Conflicts of interest

There are no conflicts to declare.

Acknowledgements

This work was supported by grants from the University of Buenos Aires (UBACyT 20020130100380), the Deutsche Forschungsgemeinschaft (DFG) (SFB 1140 and FOR 2036), CONICET and DAAD stipends, the DAAD transnational education (TNB) project between the Universities of Freiburg and Buenos Aires (TREAM), the DFG SFB850 projects Z1 and the BMBF including the framework of the e:Med research and funding

concept (FKZ 01ZX1409B). The authors would like to thank Dra. Lidia Piehl for teaching us the use of EPR, and the microarray unit of the DKFZ Genomics and Proteomics Core Facility for their related service (Dr Melanie Bewerunge-Hudler and Dr Stephan Wolf).

Notes and references

1 Y. Nose, E. M. Rees and D. J. Thiele, Structure of the Ctr1 copper trans'PORE'ter reveals novel architecture, *Trends Biochem. Sci.*, 2006, **31**, 604.
2 H. Gunshin, B. Mackenzie, U. V. Berger, Y. Gunshin, M. F. Romero, W. F. Boron, S. Nussberger, J. L. Gollan and M. A. Hediger, Cloning and characterization of a mammalian proton-coupled metal-ion transporter, *Nature*, 1997, **388**, 482.
3 S. Lutsenko, N. Barnes, Y. Bartee Mee and O. Dmitriev, Function and Regulation of Human Copper-Transporting ATPases, *Physiol. Rev.*, 2007, **87**, 1011.
4 L. Banci, I. Bertini, S. Ciofi-Baffoni, T. Kozyreva, K. Zovo and P. Palumaa, Affinity gradients drive copper to cellular destinations, *Nature*, 2010, **465**, 645.
5 P. Gow, R. Smallwood, P. Angus, A. Smith, A. Wall and R. Sewell, Diagnosis of Wilson's disease: an experience over three decades, *Gut*, 2000, **46**, 415.
6 E. A. Roberts and M. L. Schilsky, Diagnosis and Treatment of Wilson's Disease: An Update, *Hepatology*, 2008, **47**, 2089.
7 G. Multhaup, A. Schlicksupp, L. Hesse, D. Beher, T. Ruppert, C. L. Masters and K. Beyreuther, The Amyloid Precursor Protein of Alzheimer's Disease in the Reduction of Copper(II) to Copper(I), *Science*, 1996, **271**, 1406.
8 S. Bucossi, M. Ventriglia, V. Panetta, C. Salustri, P. Pasqualetti, S. Mariani, M. Siotto, P. M. Rossini and R. Squitti, Copper in Alzheimer's Disease: A Meta-Analysis of Serum, Plasma, and Cerebrospinal Fluid Studies, *J. Alzheimer's Dis.*, 2011, **24**, 175.
9 S. Ayton, P. Lei and A. I. Bush, Metallostasis in Alzheimer's disease, *Free Radical Biol. Med.*, 2013, **62**, 76.
10 R. Squitti, Copper subtype of Alzheimer's disease (AD): meta-analyses, genetic studies and predictive value of non-ceruloplasmim copper in mild cognitive impairment conversion to full AD, *J. Trace Elem. Med. Biol.*, 2014, **28**, 482.
11 A. A. Aboud, A. M. Tidball, K. K. Kumar, M. D. Neely, B. Han, K. C. Ess, C. C. Hong, K. M. Erikson, P. Hedera and A. B. Bowman, PARK2 patient neuroprogenitors show increased mitochondrial sensitivity to copper, *Neurobiol. Dis.*, 2015, **73**, 204.
12 S. Dell'Acqua, V. Pirota, C. Anzani, M. M. Rocco, S. Nicolis, D. Valensin, E. Monzani and L. Casella, Reactivity of copper-α-synuclein peptide complexes relevant to Parkinson's disease, *Metallomics*, 2015, **7**, 1091.
13 Y. Okita, A. N. Rcom-H'cheo-Gauthier, M. Goulding, R. S. Chung, P. Faller and D. L. Pountney, Metallothionein, Copper and Alpha-Synuclein in Alpha-Synucleinopathies, *Front. Neurosci.*, 2017, **11**, 114.
14 H. Fenton, Oxidation of tartaric acid in presence of iron, *J. Chem. Soc., Trans.*, 1894, **65**, 899.
15 F. Haber and J. Weiss, The catalytic decomposition of hydrogen peroxide by iron salts, *Proc. R. Soc. London, Ser. A*, 1934, **147**, 332.
16 B. Halliwell and S. Chirico, Lipid peroxidation: its mechanism, measurement, and significance, *Am. J. Clin. Nutr.*, 1993, **57**, 7155.
17 N. Arnal, M. J. de Alaniz and C. A. Marra, Cytotoxic effects of copper overload on human-derived lung and liver cells in culture, *Biochim. Biophys. Acta*, 2012, **1820**, 931.
18 R. Musacco Sebio, N. Ferrarotti, C. Saporito Magriñá, J. Semprine, H. Torti, A. Boveris, M. Castro Parodi, A. Damiano and M. G. Repetto, Rat liver antioxidant response to iron and copper overloads, *J. Inorg. Biochem.*, 2014, **137**, 94.
19 J. Semprine, N. Ferrarotti, R. Musacco Sebio, C. Saporito Magriñá, J. Fuda, H. Torti, M. Castro Parodi, A. Damiano, A. Boveris and M. G. Repetto, Brain antioxidant response to iron and copper acute intoxications in rats, *Metallomics*, 2014, **6**, 2083.
20 R. J. Sokol, M. W. Devereaux, K. O'Brien, R. A. Khandwala and J. P. Loehr, Abnormal hepatic mitochondrial respiration and cytochrome C oxidase activity in rats withlong-term copper overload, *Gastroenterology*, 1993, **105**, 178.
21 A. S. Sansinanea, S. I. Cerone, S. A. Streitenberger, C. García and N. Auza, Oxidative effect of hepatic copper overload, *Acta Physiol., Pharmacol. Ther. Latinoam.*, 1998, **48**, 25.
22 D. Ozcelik, R. Ozaras, Z. Gurel, H. Uzun and S. Aydin, Copper-mediated oxidative stress in rat liver, *Biol. Trace Elem. Res.*, 2003, **96**, 209.
23 D. Ozcelik and H. Uzun, Copper Intoxication; Antioxidant Defenses and Oxidative Damage in Rat Brain, *Biol. Trace Elem. Res.*, 2009, **127**, 45.
24 N. Arnal, L. Dominici, M. J. Tacconi de Alaniz and C. A. Marra, Copper-induced alterations in rat brain depends or route of overload and basal copper levels, *Nutrition*, 2013, **30**, 96.
25 S. Sinha, R. Christopher, G. R. Arunodaya, L. K. Prashanth, G. Gopinath, H. S. Swamy and A. B. Taly, Is low serum tocopherol in Wilson's disease a significant symptom?, *J. Neurol. Sci.*, 2005, **228**, 121.
26 S. Liang and J. Hong-Fang, Adjunctive vitamin E treatment in Wilson disease and suggestions for future trials, *Hepatology*, 2007, **51**, 1864.
27 A. Lloret, M. C. Badía, N. J. Mora, F. V. Pallardó, M. D. Alonso and J. Viña, Vitamin E paradox in Alzheimer's disease: it does not prevent loss of cognition and may even be detrimental, *J. Alzheimer's Dis.*, 2009, **17**, 143.
28 G. J. Brewer, Why vitamin E therapy fails for treatment of Alzheimer, *J. Alzheimer's Dis.*, 2011, **19**, 27.
29 I. Vermes, C. Haanen, H. Steffens-Nakken and C. Reutelingsperger, A novel assay for apoptosis, flow cytometric detection of phosphatidylserine expression on early apoptotic cells using fluorescein labelled annexin V, *J. Immunol. Methods*, 1995, **184**, 39.
30 S. Burow and G. Valet, Flow-cytometric characterization of stimulation, free radical formation, peroxidase activity and

phagocytosis of human granulocytes with 2,7-dichlorofluorescein (DCF), *Eur. J. Cell Biol.*, 1987, **43**, 128.
31 A. L. Shapiro, E. Viñuela and J. V. Maizel Jr, Molecular weight estimation of polypeptide chains by electrophoresis in SDS-polyacrylamide gels, *Biochem. Biophys. Res. Commun.*, 1967, **28**, 815.
32 N. Marks, M. J. Berg, A. Guidotti and M. Saito, Activation of caspase-3 and apoptosis in cerebellar granule cells, *J. Neurosci. Res.*, 1988, **52**, 334.
33 G. L. Ellman, Tissue sulfhydryl groups, *Arch. Biochem. Biophys.*, 1959, **82**, 70.
34 C. Saporito Magriñá, C. Borner, M. Börries and G. Andrieux, *Expression data in BEAS-2B cells and HCT116 cells incubated with copper(II) for different times*, NCBI's Gene Expression Omnibus, 2018, https://www.ncbi.nlm.nih.gov/geo/query/acc.cgi?acc=GSE109375.
35 D. Skoog, D. West, F. Holler and S. Crouch, *Química Analítica*, McGraw-Hill, México, 2001.
36 M. M. Bradford, Rapid and sensitive method for the quantitation of microgram quantities of protein utilizing the principle of protein-dye binding, *Anal. Biochem.*, 1976, **72**, 248.
37 L. Quintanar, J. A. Domínguez-Calva, E. Serebryany, L. Rivillas-Acevedo, C. Haase-Pettingell, C. Amero and J. A. King, Copper and Zinc Ions Specifically Promote Nonamyloid Aggregation of the Highly Stable Human γD Crystallin, *ACS Chem. Biol.*, 2016, **11**, 263.
38 D. P. Jones, Radical-free biology of oxidative stress, *Am. J. Physiol.: Cell Physiol.*, 2008, **295**, C849.
39 R. Franco and J. A. Cidlowski, Glutathione Efflux and Cell Death, *Antioxid. Redox Signaling*, 2012, **17**, 1694.
40 R. Ruffman and A. Wendel, GSH rescue by *N*-acetylcysteine, *Klin. Wochenschr.*, 1991, **69**, 857.
41 M. Schwarzländer, T. P. Dick, A. J. Meyer and B. Morgan, Dissecting redox biology using fluorescent protein sensors, *Antioxid. Redox Signaling*, 2016, **24**, 680.
42 M. E. Aliaga, C. López-Alarcón, R. Bridi and H. Speisky, Redox-implications associated with the formation of complexes between copper ions and reduced or oxidized glutathione, *J. Inorg. Biochem.*, 2016, **154**, 78.
43 J. Calvo, H. Jung and G. Meloni, Copper metallothioneins, *IUBMB Life*, 2017, **69**, 236.
44 Z. Xiao, J. Brose, S. Schimo, S. M. Ackland, S. La Fontaine and A. G. Wedd, Unification of the copper(I) binding affinities of the metallo-chaperones Atx1, Atox1, and related proteins: detection probes and affinity standards, *J. Biol. Chem.*, 2011, **286**, 11047.
45 M. T. Morgan, L. A. H. Nguyen, H. L. Hancock and C. J. Fahrni, Glutathione limits aquacopper(I) to sub-femtomolar concentrations through cooperative assembly of a tetranuclear cluster, *J. Biol. Chem.*, 2017, **292**, 21558.
46 R. C. Taylor, K. M. Berendzen and A. Dillin, Systemic stress signalling: understanding the cell nonautonomous control of proteostasis, *Nat. Rev. Mol. Cell Biol.*, 2014, **15**, 211.
47 V. Jovaisaite, L. Mouchiroud and J. Auwerx, The mitochondrial unfolded protein response, a conserved stress response pathway with implications in health and disease, *J. Exp. Biol.*, 2014, **217**, 137.
48 M. B. Schaaf, T. G. Keulers, M. A. Vooijs and K. M. Rouschop, LC3/GABARAP family proteins: autophagy-(un)related functions, *FASEB J.*, 2016, **30**, 3961.
49 A. Krężel and W. Maret, The biological inorganic chemistry of zinc ions, *Arch. Biochem. Biophys.*, 2016, **611**, 3.
50 K. Nakamura, F. Endo, T. Ueno, H. Awata, A. Tanoue and I. Matsuda, Excess Copper and Ceruloplasmin Biosynthesis in Long-term Cultured Hepatocytes from Long-Evans Cinnamon (LEC) Rats, a Model of Wilson Disease, *J. Biol. Chem.*, 1995, **270**, 7656.
51 H. Sies, Oxidative stress: a concept in redox biology and medicine, *Redox Biol.*, 2015, **4**, 180.
52 A. Gupte and R. J. Mumper, Elevated copper and oxidative stress in cancer cells as a target for cancer treatment, *Cancer Treat. Rev.*, 2009, **35**(1), 32.
53 B. An, R. H. Goldfarb, R. Siman and Q. P. Dou, Novel dipeptidyl proteasome inhibitors overcome Bcl-2 protective function and selectively accumulate the cyclin-dependent kinase inhibitor p27 and induce apoptosis in transformed, but not normal, human fibroblasts, *Cell Death Differ.*, 1998, **5**, 1062.
54 P. Vassilyadi, S. V. Harding, E. Nitschmann and L. J. Wykes, Experimental colitis and malnutrition differentially affect the metabolism of glutathione and related sulfhydryl metabolites in different tissues, *Eur. J. Nutr.*, 2016, **55**, 1769.
55 K. E. Sant, J. M. Hansen, L. M. Williams, N. L. Tran, J. V. Golstone, J. J. Stegeman, M. E. Hahn and A. Timme-Laragy, The role of Nrf1 and Nrf2 in the regulation of glutathione and redox dynamics in the developing zebrafish embryo, *Redox Biol.*, 2017, **13**, 207.
56 Y. Hatori, Y. Yan, K. Schmidt, E. Furukawa, N. M. Hasan, N. Yang, C. N. Liu, S. Sockanathan and S. Lutsenko, Neuronal differentiation is associated with a redox-regulated increase of copper flow to the secretory pathway, *Nat. Commun.*, 2016, **7**, 10640.
57 L. Mosoni, D. Breuillé, C. Buffière, C. Obled and P. P. Mirand, Age-related changes in glutathione and skeletal muscle carbonyl content in healthy rats, *Exp. Gerontol.*, 2004, **39**, 203.

